EUROPEAN ORGANIZATION FOR NUCLEAR RESEARCH

FURTHER EVIDENCE FOR PRODUCTION OF ELECTRONS WITH SMALL TRANSVERSE MOMENTA IN pp COLLISIONS

M. Block, A. Böhm, F. Ceradini, D. DiBitonto,
J. Irion, A. Kernan, J. Layter, F. Muller, A. Nakkasyan,
B. Naroska, F. Navach, M. Nussbaum*), A. Orkin-Lecourtois**),
C. Rubbia, M. Sachwitz, D. Schinzel, H. Seebrunner,
B. Shen, A. Staude, R. Tirler, G. Van Dalen and R. Voss

III. Physikalisches Institut der Technischen Hochschule***)
Aachen, Germany

University of California, Riverside, Calif., USA†)

CERN, Geneva, Switzerland

Harvard University, Cambridge, Mass., USA

Sektion Physik der Universität, Munich, Germany***)

Northwestern University, Evanston, Ill., USA†)

ABSTRACT

A new measurement of prompt lepton production at small transverse momenta in pp collisions at the ISR, for $\sqrt{s}$ = 53 GeV, is presented. The e/π ratio, which is about 10^{-4} for p_T > 1 GeV/c, rises rapidly as p_T goes to smaller values, confirming our original results. The data are consistent with equality between the numbers of e^+ and e^- produced in each transverse momentum interval.

Geneva - 10 August 1977

(Submitted to Nuclear Physics B)

---

*) Permanent address: Physics Dept., University of Cincinnati, Cincinnati, Ohio, USA.

**) Supported by LAL, Orsay, France.

***) Supported by the Bundesministerium für Forschung und Technologie, Germany.

†) Supported by the Energy Research and Development Agency, USA.

Over the last few years prompt lepton production in proton-proton (or proton-nucleus) collisions has been extensively studied at various centre-of-mass energies from 4.5 to 53 GeV [1]. In the central region ($x \approx 0$) and at large (> 1 GeV/c) values of the lepton transverse momentum p_T, measurements at FNAL and at the CERN ISR are in agreement on the lepton/pion ratio:

$$\frac{\mu^{\pm}}{\pi} \approx \frac{e^{\pm}}{\pi} \approx 10^{-4} \ .$$

Also it appears that most of the effect (and possibly all of it above $p_T \approx 2$ GeV/c) can be ascribed to vector-meson ($\rho,\omega,\psi/J$) production [2].

Four experiments have produced electron data in the central region and at smaller values of the lepton transverse momentum ($p_T < 1$ GeV/c). An experiment done at the ISR by this collaboration [3] shows a strong rise of the e/π ratio as p_T decreases below 1 GeV/c. Another ISR experiment [4], at slightly higher p_T values might suggest a decrease in the ratio, although both experiments agree for $p_T \gtrsim 1$ GeV/c. At lower energies, an experiment at BNL [5], down to $p_t = 0.5$ GeV/c, finds an increase similar to the one observed in Ref. 3, while an early measurement at the CERN PS [6] found no evidence for electron production at $p_T = 0.5$ GeV/c.

In view of the importance of this low p_T region, where some new dynamical mechanism, such as charmed particle production or low-mass lepton pairs, must be invoked to explain a copious yield of prompt leptons, we have performed a new experiment with an improved detector in order to verify the results of our previous experiment [3]. This experiment is part of a comprehensive search for charm production at the ISR, other results of which have already been published [7,8].

The set-up (Fig. 1), like the previous one, consists of a magnetic spectrometer (Fig. 1a) of 0.6 T·m bending power, located at 32° from one of the ISR beams and covering a 0.02 sr solid angle. The energy was $\sqrt{s} = 53$ GeV. Electrons are distinguished from hadrons by requiring a pulse in a 1.1 m long threshold Čerenkov counter filled with CO_2 at atmospheric pressure, and by checking that the measured momentum is equal to the energy deposited in a 3×5 matrix of lead-glass Čerenkov counters 15 radiation lengths deep.

For reconstructing trajectories of particles and measuring their momenta, we have replaced the drift chambers of Ref. 3 by proportional chambers of 2 mm wire spacing. These chambers, previously used in another ISR experiment [9], have excellent efficiency and multitrack capability, and allow a high data-taking rate (about 250 events/sec written on video tape). Four modules, each consisting of four planes with wires at 0°, ±45°, and 90° from the vertical direction, placed two in front and two behind the magnet, yield a more than adequate momentum accuracy ($\Delta p/p = 1.2\%$ at 1 GeV/c, whereas $\Delta E/E = 14\%$ in the lead-glass at the same momentum).

Three layers of dE/dx scintillation counters, two in front and one behind the magnet, are used for triggering purposes; at the analysis stage their recorded pulse heights provide rejection of small-angle electron pairs. Approximately 99% of the larger angle pairs are tagged by the presence of a pulse in an array of guard counters around the front trigger counters. Figure 2a shows the geometrical layout of these counters (which is somewhat different from that used in the experiment of Ref. 3).

The present vacuum chamber (Fig. 2b) in Intersection I-6 of the ISR differs considerably from the one used in the previous experiment. The current chamber is a cylinder with a uniformly thick 0.3 mm stainless steel wall, while the bicone used previously had wall thicknesses of 0.2 and 0.7 mm in its central and forward parts, respectively. This, together with the different shape of the wall corrugations, results in an average thickness of 0.7 mm along the direction of the spectrometer axis, in contrast with thicknesses of 0.45 and 1.5 mm for the thin and thick parts of the previous bicone.

The change in vacuum chamber geometry strongly influences the amount of Compton and conversion-pair electrons entering the spectrometer, while the modification of the geometry of the guard counters results in a different probability for Dalitz and conversion electrons to be recorded as single electrons. Thus the total electron signal should be different from that found in Ref. 3, but the signal remaining after subtraction of all backgrounds should be the same in both experiments.

The experimental procedure is the following. We measure, in various p_T intervals and for both signs of charge, the total number N_e of electrons and N_h of hadrons detected in the same (small) solid angle around the c.m. angle $\theta = 32°$. We then compute the ratio n_e/n_π, where n_π is the pion content of n_h, and n_e and n_h are rates obtained by normalizing N_e and N_h to a fixed number of counts in a monitor whose counting rate is proportional to the rate of pp interactions. In this way, absolute evaluation of integrated luminosities is not necessary, and the ratio is independent of geometrical acceptance. To correct for detection efficiencies $\varepsilon_e, \varepsilon_\pi$ for electrons and pions, we need know only the relative efficiency $\varepsilon = \varepsilon_e/\varepsilon_\pi$. By imposing the same trigger requirements and analysis criteria in the detectors common to both the electrons and the pions (scintillation counters and proportional chambers), we reduce ε to the detection efficiency for electrons in the specialized electron detectors (gas Čerenkov counter and lead-glass matrix).

Separate triggers were used to record N_e and N_h. Both triggers required a threefold coincidence between the two counters before the magnet and the one behind it. In addition, the electron trigger required a pulse in the gas Čerenkov

counter and a total energy deposition greater than 0.2 GeV in the lead-glass matrix. This is well below the energy corresponding to the lowest p_T value (p_T = 0.2 GeV/c, hence E ≈ 0.4 GeV) in the final sample.

In the analysis stage, the following conditions are imposed on particles in both trigger modes:

i) pulse heights in the coincidence counters compatible with minimum ionization;

ii) no hit in the guard counters;

iii) one track only in the proportional chambers, which extrapolates back to the interaction region of the ISR;

iv) only one cluster in the lead-glass matrix, whose centre is compatible with the extrapolation of the track.

These requirements, applied to the hadron trigger, define the hadron sample. From the electron trigger mode, we extract the electron sample by further requiring that:

v) the Čerenkov pulse be greater than a threshold corresponding to about 1.5 photoelectrons;

vi) the energy measured in the lead-glass be equal within errors to the momentum measured in the spectrometer.

Quantitatively, these last two requirements imposed on the electron sample translate into a measured 80% relative electron/pion detection efficiency, ε. Conversely, the probability for a hadron to survive these cuts, and thus be wrongly identified as an electron, is found to decrease from 0.9×10^{-4} for $0.2 < p_T < 0.3$ GeV/c to 0.03×10^{-4} for $p_T \approx 1$ GeV/c. These numbers have been evaluated from the spectra of Čerenkov and lead-glass pulses obtained with the hadron trigger mode.

For each p_T interval the e/π ratio is arrived at in the following way:

a) For both electron and hadron trigger modes, the direction of the magnetic field was periodically reversed. Consequently, the rate for a given particle, h^+ for example, is given by

$$n_{h^+} = \frac{N_{h^+}^{\uparrow}}{M^{\uparrow}} + \frac{N_{h^+}^{\downarrow}}{M^{\downarrow}} ,$$

where $N_{h^+}^{\uparrow}, N_{h^+}^{\downarrow}$ are the numbers of positive hadrons accepted in the periods corresponding to the total numbers of monitor counts $M^{\uparrow}, M^{\downarrow}$, for each direction of the magnetic field in the spectrometer. This procedure ensures equality of acceptances for e^+ and e^-, and for h^+ and h^-, provided their angular distributions are approximately the same over the angular opening of the telescope, as they were found to be.

b) To get the pion rate, the hadron rate is multiplied by the pion/(pion + kaon + proton) ratio. Each component in this expression has been determined experimentally[10,11] and is weighted by its relative detection efficiency as deduced from the minimum ionization requirement in the trigger counters. This favours pions over kaons and protons, especially in the low p_T region. Thus the pion/hadron ratio, $r^{\pm}$, is found to decrease from 0.99 at p_T = 0.2 GeV/c to about 0.75 (0.65) at p_T = 1 GeV/c for negative (positive) particles. The measured rates of pions are then given by $n_{\pi^{\pm}} = (n_{h^{\pm}})r^{\pm}$ and, since we find $n_{\pi^+} \approx n_{\pi^-}$, we define $n_{\pi} = (n_{\pi^+} + n_{\pi^-})/2 \approx n_{\pi^0}$.

c) With this definition of the pion rate, the e/π ratio in each p_T interval is given by

$$\frac{e^{\pm}}{\pi} = \frac{n_{e^{\pm}}}{\varepsilon n_{\pi}} ,$$

where $\varepsilon = 0.80$ is the correction factor for relative electron/pion detection efficiency discussed earlier.

The values of the total measured $e^{\pm}/\pi$ ratio are listed in Table 1 and the numbers obtained for e^{+}/π are displayed in Fig. 3a. As anticipated, these results are substantially different from those of the previous experiment[3]. To interpret these new results, we must first evaluate the background contribution from well-understood sources of electrons.

i) Electrons and positrons pair-produced by real photons in the vacuum chamber wall

At the time of production, the pairs have an opening angle which is essentially zero, and thus they should be eliminated by the single-particle requirement. However, the low energy member of a very energy-asymmetrical pair may be multiple-scattered by the vacuum chamber wall through an angle large enough to miss even the guard counters, so that the high energy member is recorded as a single electron. The resulting contribution to e/π has been calculated by a Monte Carlo program, which we describe in some detail here, since its main features are used for the other background sources.

The initial pions are generated according to the experimental[10,11] distribution $d^3\sigma/dp_T dy d\phi \propto p_T e^{-bp_T}$, with $b = 5.4\ (GeV/c)^{-1}$; and their points of origin in the ISR diamond are given the known density distribution of the interactions. Among the charged pions so generated, those accepted through the magnetic spectrometer (according to the same criteria used in the analysis of real events) reproduce our measured spectra very well. The neutral pions generated with the same distribution and intensity are allowed to decay isotropically into two photons. Each photon produces a pair at a random point along its path in the vacuum chamber

wall, whose mathematical description reproduces the corrugations. The pair is given a weight proportional to the potential thickness traversed by the photon. The energies of the two electrons are generated according to the Bethe-Heitler formula[12] and their multiple scattering inside the wall is followed through a random-walk process, correlated in both displacement and angle, until they leave the wall. An electron is accepted if it goes through the whole spectrometer, while its companion misses the trigger and guard counters. The results of the Monte Carlo program agree very well with the relation $e^{\pm}/\pi = A/p_T^2$, which results from a simple analytical calculation shown in Appendix A.

However, since the constant A depends quite sensitively on the scattering law and on the actual geometry of the chamber wall, we designed an ancillary experiment to measure directly the e/π ratio due to conversion electrons. This experiment employs a dummy wall, identical to the vacuum chamber wall, from which it is separated by an array of thin anticoincidence counters (Fig. 2b). The same triggers and the same analysis criteria were used as in the main experiment, but single electrons so detected were retained only if there was no hit in the anticoincidence counter crossed by the (extended) electron track, ensuring that the electron originated from a neutral primary, presumably a γ-ray from meson decay. This procedure permits the direct measurement of the rates of e^+ and e^- produced by γ interactions in the vacuum chamber wall*); the experimental e^+/π ratio is found to follow the predicted $1/p_T^2$ law. Incidentally, this is a check of the constancy of electron detection efficiency versus p_T.

The results of the Monte Carlo pair-production program, corrected for the average energy loss due to radiation (see Appendix B), and the results from the dummy wall experiment**) for positrons (Table 1) agreed both in shape and magnitude, each exhibiting a $1/p_T^2$ behaviour. The absolute agreement in the low p_T region was within 3%, a result which gives us confidence that the Monte Carlo conditions imposed faithfully reflected the true experimental conditions. Figure 3a shows, as a function of p_T, the e^+/π ratios for (a) the total detected signal and (b) the signal from the dummy wall experiment (conversion positrons) along with its $1/p_T^n$

---

*) In the experiment with anticounters and dummy wall, some of the pair and Compton electrons created in the last mm or so of the counter thickness give no pulse in the counter and are thus wrongly counted as wall-produced $e^{\pm}$. To correct for this effect, the same experiment was run with the dummy wall removed, and the corresponding $e^{\pm}/\pi$ values subtracted from the $e^{\pm}/\pi$ values found with the wall in place.

**) The dummy wall results have undergone a small geometric correction, which is discussed in Appendix A.

fit. The best value of n was found to be 2.05, compatible with a $1/p_T^2$ law. These fitted values, except for the interval*) $0.2 < p_T < 0.3$ GeV/c, were used for background subtraction.

ii) Electrons from Compton effect

Their contribution is evaluated by the same Monte Carlo program, using the Klein-Nishina formula[13] to generate the angle and energy of the electron. The calculated e^-/π values also follow an approximate $1/p_T^2$ law, which again can be deduced from a simple analytical calculation. The dummy wall experiment measures for e^- the sum of both Compton and conversion electrons. Indeed, it is seen from Table 1 that the dummy wall e^-/π ratios are larger than the corresponding e^+/π ratios. The differences of the two measurements are compatible with the Monte Carlo values calculated for the Compton effect. The $1/p_T^n$ fit to the measured e^-/π values from the dummy wall was used for background subtraction*).

iii) Electrons originating from π^0 and η^0 Dalitz decays and from kaon decays

Electrons from Dalitz pairs and from $e\pi\nu$ decays of charged and neutral kaons can be evaluated only by means of Monte Carlo programs. The good agreement between the Monte Carlo predictions and the measured values of the $e^\pm$ rates due to photon interactions, plus the fact that scattering in the wall plays a smaller role in these cases than for other sources of background**) are reasons to believe in the validity of the Monte Carlo results for Dalitz and K_{e3} decays. In the programs the primary hadrons were generated according to the law $d^3\sigma/dp_T dy d\phi \propto Ap_T e^{-bp_T}$, where A = 1, 0.11, 0.067 (0.047) and b = 5.4, 4.5, 4.8 $(GeV/c)^{-1}$ for π, η, $K^+(K^-)$, respectively, as indicated by available experimental data[10,11,14]. The K_S^0 production cross-section is assumed to be equal to $\frac{1}{2}(\sigma_{K^+} + \sigma_{K^-})$. Dalitz pairs are

*) The acceptance of the first interval $0.2 < p_T < 0.3$ GeV/c is markedly non-uniform over the interval, owing to the large bending of 0.4 GeV/c particles in our magnet. Thus, we treat it separately, subtracting the actual experimental value given by the dummy wall.

**) Background due to Dalitz pairs, like background due to γ conversion, arises whenever one of the pair, emerging at a large angle, escapes detection by the counter system. However, in the Dalitz case, the initial pair-producing process results in a wide angular distribution with a slowly falling tail at large angles, and scattering in the wall only slightly broadens this distribution. Furthermore, the variation due to the wall corrugations in the thickness t of iron traversed by the electrons induces a much less pronounced modulation in the Dalitz-pair background contribution than in the γ-conversion case, since the effect goes as $t^{1/2}$ for Dalitz and as $t^{3/2}$ for γ conversion. In fact, the Monte Carlo results indicate that the Dalitz-pair contribution to the background decreases by about 20% when scattering in the wall is turned off.

generated according to the Kroll-Wada formula[15] and K_{e3} decays from a V-A matrix element. Results for the e^+/π ratio from these sources, corrected for radiation losses (see Appendix B), are displayed in Fig. 3b, together with the measured e^+/π residual signal (obtained by subtracting from the total measured e^+/π ratio the value of e^+/π obtained from the dummy wall experiment). It is apparent that the backgrounds decrease with p_T faster than the residual signal, and that even at the lowest p_T values, their sum is smaller than the signal.

Table 1 summarizes all experimental data and the Monte Carlo results (Dalitz and kaon) used for background subtraction. Table 2 gives the $e^{\pm}/\pi$ values after subtraction of all backgrounds from the measured e/π signal. The values of the difference $(e^- - e^+)/2\pi$, also tabulated, fluctuate around zero and are compatible with it, as illustrated in Fig. 4a. Assuming the equality of the e^+/π, e^-/π ratios we calculate their weighted average, e/π. Table 2 and Fig. 4b display these final values of e/π, where the quoted errors are purely statistical and the results are not corrected for radiation losses (see Appendix B).

We note at this point that these measured values of e/π are not truly the ratios of inclusive yields of electrons and pions. In order to suppress electrons from pairs, we necessarily rejected not only those electrons, but also all single electrons which were accompanied by a second particle in the solid angle defined by the guard and trigger counters. For consistency, the same restrictions were applied to the pions. Clearly the true inclusive yields are larger than those we measured, by factors which could easily be different for electrons and pions, since they presumably arise from different classes of interactions. In order to estimate this effect, we reanalysed the data, suppressing part of the guard counter information from the anticoincidence requirement, thus experimentally reducing the solid angle for detection of a second particle. Both the electron and the pion signal increased, but after a larger electron background subtraction, the final e/π values were found to be equal, within errors, to those obtained in the original analysis*). Thus we find that losses from this source affect both electrons and pions in approximately the same way.

It is seen from Table 2 and Fig. 4b that the e/π values for direct electron production show a marked increase when p_T decreases from 1 GeV/c to $\sim$ 0.3 GeV/c, consistent with an approximate $1/p_T$ behaviour in this transverse momentum interval, in agreement with the original findings of Ref. 3.

There has been considerable speculation concerning the origin of direct leptons. The possibility that leptonic decay of the charmed D(1.87) meson contributes to direct lepton production has been extensively studied[2,16], and theoretical

*) More precisely, dividing the data in two p_T intervals ($0.2 < p_T < 0.5$ GeV/c and $0.5 < p_T < 1$ GeV/c) we find in each of those intervals an e/π value equal to the original one, with a statistical error of ±14%.

attempts to reproduce our data with decay schemes $D \to e + \nu + K + \ldots$ have led to cross-section × branching ratio estimates from 30 to 150 μb. If we take a branching ratio[8,17] of 10%, these estimates imply total cross-sections of 0.3-1.5 mb, a result barely consistent with our measured upper limit of 8 μb for $\sigma \cdot B(D^0 \to K^{\mp}\pi^{\pm})$ at $\sqrt{s}$ = 53 GeV [7], when we take into account the experimental estimate of the branching ratio for $D^0 \to K^{\mp}\pi^{\pm}$ [18].

The possibility of an electromagnetic origin for the direct electrons is suggested by the observed equality of e^+ and e^-, in each momentum interval. A mechanism for single photon production, and hence, production of massive electron pairs from virtual photons, has been suggested[19], which could explain the observation of direct electrons below the charm threshold. The pair would have to be sufficiently massive so that, on the average, the opening angle would be large enough for one of the pairs to miss the guard counters (the pairs would need to be $\gtrsim$ 100 MeV in mass). For the direct electrons reported in the same p_T range, but at low $\sqrt{s}$ values, from 4.5 to 6.9 GeV [20], the authors tend to rule out pairs of small invariant masses, whereas they might be expected to be more copious than those of higher mass. Thus, the origin of the mechanism for direct electron production at low p_T is not yet established.

We wish to thank the ISR Division for their efficient cooperation in installing the experiment and Professor L. Van Hove for encouraging discussions. One of us (M.N.) expresses his gratitude to the EP Division and Dr. E. Picasso for enabling him to participate.

REFERENCES

1) See, for example, L. Lederman, Phys. Reports 26 (1976) 149.

2) M. Bourquin and J.M. Gaillard, Nuclear Phys. B114 (1976) 334-364.

3) L. Baum et al., Phys. Letters 60B (1976) 485.

4) F.W. Büsser et al., Nuclear Physics B113 (1976) 189-245.

5) E.W. Beier et al., Phys. Rev. Letters 37 (1976) 1117.

6) K. Winter, Phys. Letters 57B (1975) 479.

7) J.C. Alder et al., Phys. Letters 66B (1977) 401.

8) L. Baum et al., Phys. Letters 68B (1977) 279.

9) L. Baksay et al., Nuclear Instrum. Methods 133 (1976) 219.

10) B. Alper et al., Nuclear Physics B87 (1975) 19.

11) B. Capiluppi et al., Nuclear Physics B79 (1974) 189.

12) H.A. Bethe and W. Heitler, Proc. Roy. Soc. A146 (1934) 83.

13) O. Klein and Y. Nishina, Z. Physik, 52 (1929) 853.

14) K.J. Anderson et al., Phys. Rev. Letters 37 (1976) 805.

15) D. Kroll and W. Wada, Phys. Rev. 98 (1954) 1355.

16) I. Hinchliffe and C.H. Llewellyn Smith, Phys. Letters 61B (1976) 472.
K. Kajantie, Invited talk at the International Summer Institute for Theoretical physics, Bielefeld, 1976 (Research Institute for Theoretical Physics, Helsinki, Preprint 19-1976).
C. Ferro Fontàn and R. Odorico, A common (charm) origin for pp direct electrons and e^+e^- anomalous electron events, University of Trieste Preprint, presented at the European Conf. on Particle Physics, Budapest, July 1977.

17) M. Gaillard, B. Lee and J. Rosner, Rev. Mod. Phys. 47 (1975) 277.

18) G. Goldhaber, Talk at Summer Institute of Particle Physics, Stanford, California, August 1976 (LBL-5534).

19) G.R. Farrar and S.C. Frautschi, Phys. Rev. Letters 36 (1976) 1017.
R. Rückl, Phys. Letters 64B (1976) 39.

20) E.W. Beier et al., Phys. Rev. Letters 37 (1976) 1114.

Table 1

Measured and calculated values of e/π (in units of 10^{-4})

p_T (GeV/c)	0.2-0.3	0.3-0.4	0.4-0.5	0.5-0.6	0.6-0.7	0.7-0.8	0.8-0.9	0.9-1.0	1.0-1.2	1.2-2.0
e^- a) Signal	27.68 ± 1.70	15.13 ± 0.86	9.06 ± 0.56	6.16 ± 0.45	4.88 ± 0.43	4.32 ± 0.43	3.74 ± 0.48	2.80 ± 0.50	2.69 ± 0.43	2.40 ± 0.48
e^- a) Pair + Compton b)	14.37 ± 1.41	6.05 ± 0.88	3.99 ± 0.46	2.86 ± 0.40	2.17 ± 0.40	1.71 ± 0.38	1.40 ± 0.37	1.16 ± 0.36	0.91 ± 0.33	0.45 ± 0.24
e^- a) Residual	13.31 ± 2.21	9.08 ± 1.23	5.07 ± 0.72	3.30 ± 0.60	2.71 ± 0.59	2.61 ± 0.57	2.34 ± 0.61	1.64 ± 0.62	1.78 ± 0.54	1.95 ± 0.54
e^+ a) Signal	24.23 ± 1.55	14.21 ± 0.80	8.20 ± 0.52	5.64 ± 0.47	4.16 ± 0.36	3.74 ± 0.40	3.33 ± 0.46	3.03 ± 0.52	2.27 ± 0.42	1.79 ± 0.41
e^+ a) Pair b)	12.17 ± 1.03	4.77 ± 0.65	2.85 ± 0.32	1.89 ± 0.30	1.35 ± 0.30	1.00 ± 0.28	0.76 ± 0.26	0.62 ± 0.23	0.46 ± 0.20	0.21 ± 0.13
e^+ a) Residual	12.06 ± 1.86	9.44 ± 1.03	5.35 ± 0.61	3.75 ± 0.56	2.81 ± 0.47	2.74 ± 0.49	2.57 ± 0.53	2.41 ± 0.57	1.81 ± 0.47	1.58 ± 0.43
Hadron contamin. a)	1.10	0.52	0.15	0.10	0.05	0.04	0.04	0.05	0.07	0.10
$(\eta+\pi^0)$ Dalitz c)	6.89	2.82	1.53	0.94	0.62	0.44	0.33	0.25	0.17	0.07
K_{e3} e^- c)	0.81	0.40	0.24	0.16	0.12	0.09	0.07	0.05	0.04	0.02
K_{e3} e^+ c)	0.97	0.48	0.29	0.20	0.14	0.11	0.08	0.07	0.05	0.02

a) The errors quoted for the experimentally measured quantities are statistical only; errors on hadron contamination are small compared to errors on the residual signal.
b) Values of Compton and pair backgrounds are the results of the dummy wall experiment, fitted, above p_T = 0.3 GeV/c, to a $1/p_T^n$ law.
c) Monte Carlo values appearing in the table have been corrected for radiation losses (see Appendix B); their statistical errors, not quoted, are small with respect to the measurement errors.

Table 2

Ratios a) of prompt electrons to pions (in units of 10^{-4})

p_T (GeV/c)	0.2-0.3	0.3-0.4	0.4-0.5	0.5-0.6	0.6-0.7	0.7-0.8	0.8-0.9	0.9-1.0	1.0-1.2	1.2-2.0
e^-/π	4.51 ± 2.21	5.34 ± 1.23	3.15 ± 0.72	2.10 ± 0.60	1.92 ± 0.59	2.04 ± 0.57	1.90 ± 0.61	1.29 ± 0.62	1.50 ± 0.54	1.76 ± 0.54
e^+/π	3.10 ± 1.86	5.62 ± 1.03	3.38 ± 0.61	2.51 ± 0.56	2.00 ± 0.47	2.15 ± 0.49	2.12 ± 0.53	2.04 ± 0.57	1.52 ± 0.47	1.39 ± 0.43
$\frac{e^+-e^-}{2\pi}$	-0.70 ± 1.44	0.14 ± 0.80	0.11 ± 0.47	0.20 ± 0.41	-0.04 ± 0.38	0.05 ± 0.38	0.11 ± 0.40	0.37 ± 0.42	0.01 ± 0.36	-0.18 ± 0.35
$\frac{e^++e^-}{2\pi}$ b)	3.68 ± 1.42	5.50 ± 0.79	3.28 ± 0.47	2.32 ± 0.41	1.97 ± 0.37	2.10 ± 0.37	2.03 ± 0.40	1.70 ± 0.42	1.51 ± 0.35	1.53 ± 0.34

a) Not corrected for radiation losses -- see Appendix B.
b) Weighted average of e^+/π and e^-/π.

Figure captions

Fig. 1 : Experimental layout.

Fig. 2 : a) Disposition of the trigger and guard counters.
b) Details of the dummy wall experiment for measuring the background due to electrons from γ interactions.

Fig. 3 : a) Total e^+/π signal and background signal measured in the dummy wall experiment.
b) Residual signal (total signal minus background measured in the dummy wall) compared with Monte Carlo calculated values for other background sources.

Fig. 4 : $e^{\pm}/\pi$ values for the prompt electrons.
a) Values of the differences $(e^+ - e^-)/2\pi$.
b) Values of e/π, the weighted average of e^+/π and e^-/π.

ELECTRON SPECTROMETER

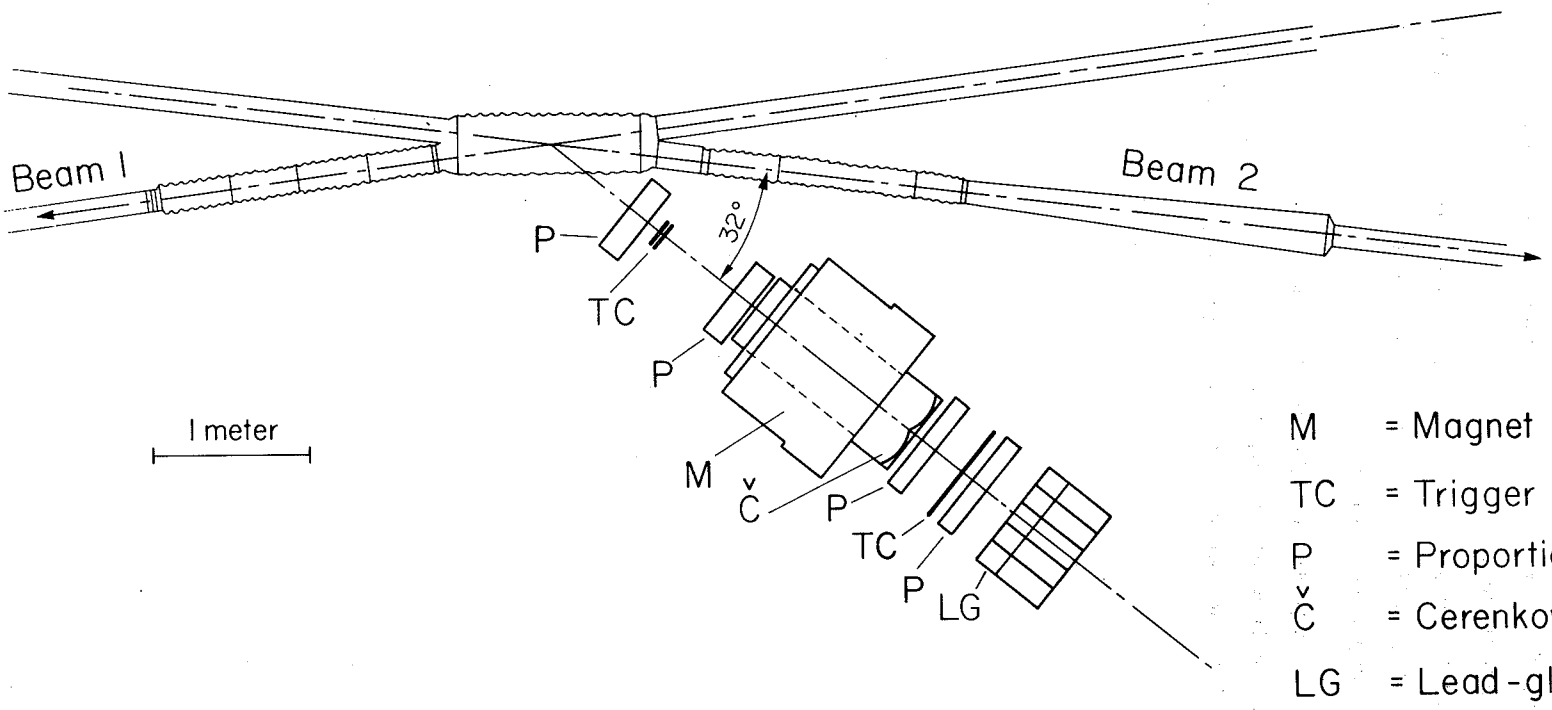

M = Magnet
TC = Trigger counters
P = Proportional chambers
C = Cerenkov - counter
LG = Lead-glass array

Fig. 1

Scintillation counter system a)

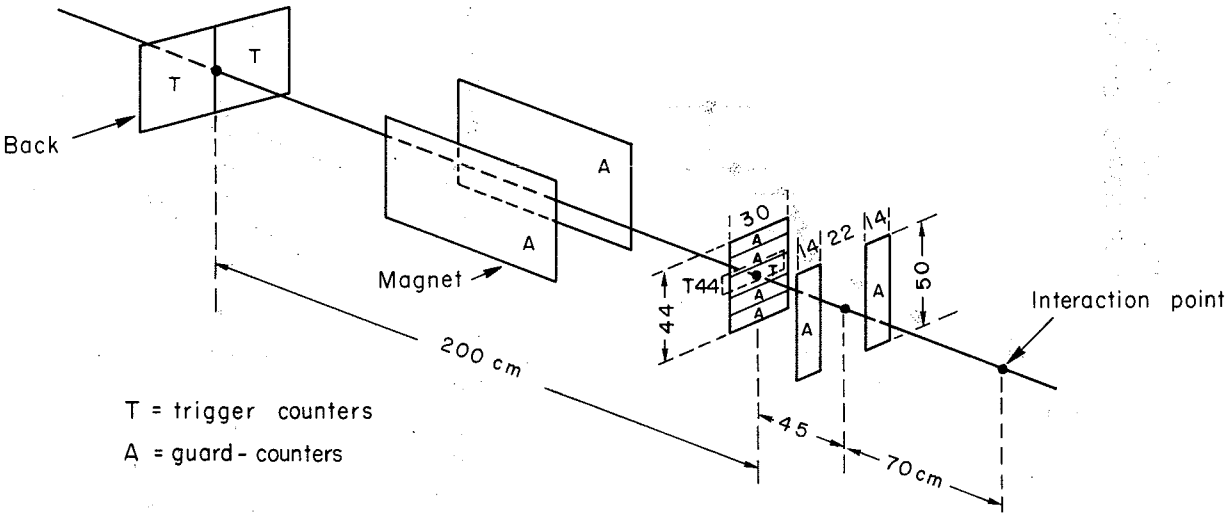

Dummy wall experiment b)

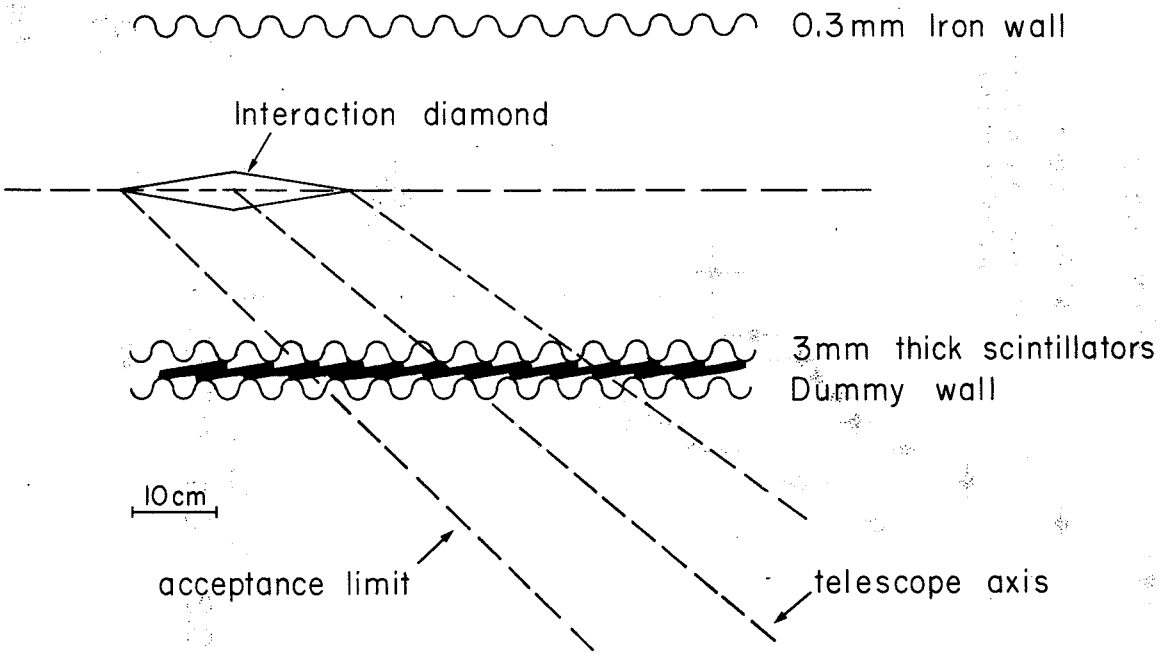

Fig. 2

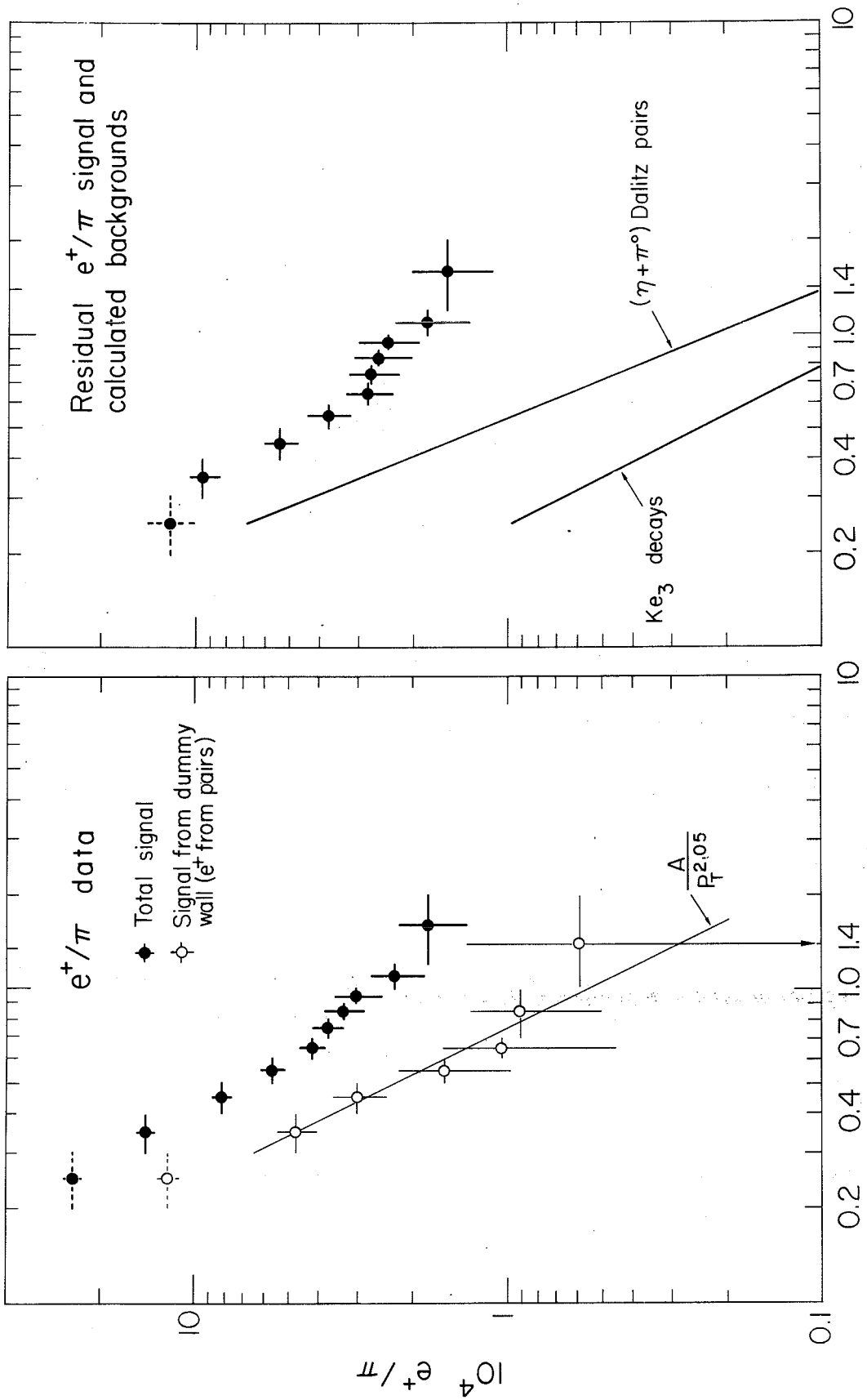
10^4 e^+/π
e^+/π data
Total signal
Signal from dummy wall (e^+ from pairs)
$\frac{A}{P_T^{2.05}}$
a)
p_T (GeV/c)
Residual e^+/π signal and calculated backgrounds
$(\eta+\pi^0)$ Dalitz pairs
Ke_3 decays
b)

Fig. 3

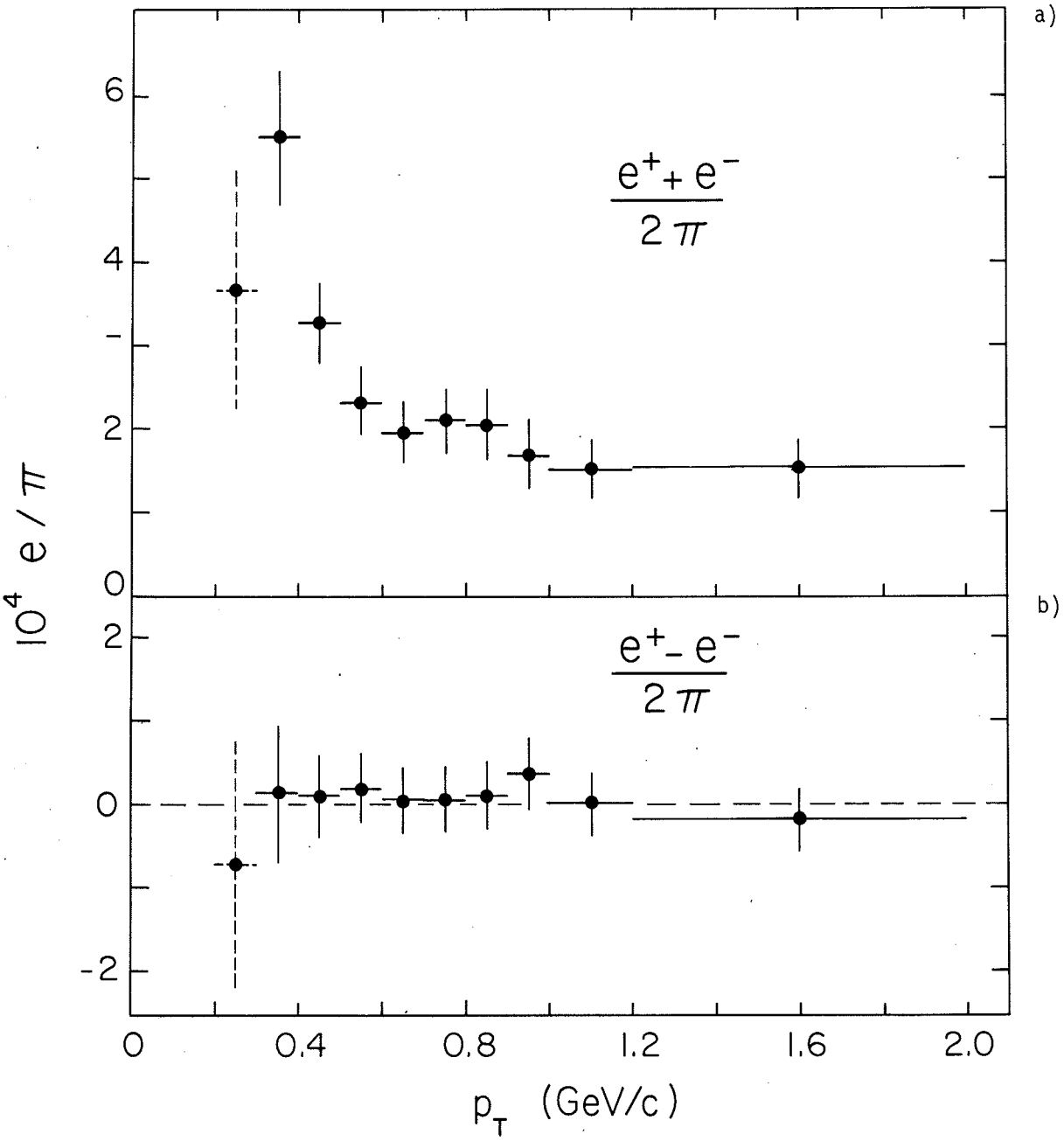
a)
b)
$\frac{e^+ + e^-}{2\pi}$
$\frac{e^+ - e^-}{2\pi}$
$10^4\ e/\pi$
6
4
2
0
2
0
-2
0
0.4
0.8
1.2
1.6
2.0
p_T (GeV/c)

Fig. 4

APPENDIX A

AN ANALYTICAL ESTIMATE OF PAIR-PRODUCTION BACKGROUND

In order to have the low-energy member (taken to be e^-) escape the guard counters, we assume that the electron must scatter through a spatial angle greater than θ_{min} (≈ 0.2 rad), the average angle subtended by the edge of the guard counters. It is simple to show that the probability $H(\theta_{min})$ for the electron to scatter through an angle $\geq \theta_{min}$ is given by

$$H\left(\theta_{min}\right) = \exp\left[-\frac{1}{2}\left(\frac{\theta_{min}}{\theta_{proj}}\right)^2\right], \tag{A.1}$$

where

$$\theta_{proj} = \frac{k}{p_e}\sqrt{t}\ , \tag{A.2}$$

t being the distance the electron travels through the vacuum chamber ($0 \leq t \leq \ell$) measured in radiation lengths, p_e the electron momentum in GeV/c, θ_{proj} the projected angle in radians, and k is the scattering constant, $k \simeq 0.015$ GeV/c. For our vacuum chamber ($\langle \ell \rangle = 0.04$ radiation lengths), the average distance traversed is ~ 0.02 radiation lengths and thus, from Eq. (A.1), $p_{e^-} \lesssim 0.02$ GeV/c for 99% of all events in which the e^- escapes the guard counters. Since the positron momentum registered as a "single" particle must exceed 0.4 GeV/c, we see that

$$p_\gamma = p^- + p^+ \approx p^+ \ . \tag{A.3}$$

Thus, the positron essentially carries off the γ-ray energy.

Experimentally, the normalized π^0 momentum spectrum is given by the law

$$dN_{\pi^0} = b^2 N_{\pi^0}\, e^{-bp_T}\, p_T\, dp_T\ , \tag{A.4}$$

where $b = 5.4\ (\text{GeV/c})^{-1}$. This in turn gives rise to a γ-ray spectrum

$$dN_\gamma = 2N_{\pi^0} b\, e^{-bp'_T}\, dp'_T\ , \tag{A.5}$$

where p'_T is the transverse momentum of the γ-ray. We re-express Eq. (A.5) in terms of the γ-ray momentum [which is p^+, because of Eq. (A.3)] at a fixed angle θ ($\approx 32^\circ$ for our experiment), and obtain

$$dN_\gamma = 2N_{\pi^0} b'\, e^{-b'p^+}\, dp^+\ , \tag{A.6}$$

where $b' \equiv b \sin\theta$.

For analytical convenience, we approximate by a flat distribution the Bethe-Heitler formula for $dG(p^-,t)$, the probability for a γ to produce, by materializing in a thickness dt, an electron of momentum p^-:

$$dG(p^-,t) = \frac{7}{9}\frac{dp^- dt}{p_\gamma} \approx \frac{7}{9}\frac{dp^- dt}{p^+} . \qquad (A.7)$$

Thus, the total number of positrons registered in our apparatus as "singles" is given by

$$dN(e^+) = dN_\gamma \int_{p^-=0}^{p^+} \int_{t=0}^{\ell} dG\, H\left(\theta_{min}\right),$$

i.e.

$$dN(e^+) = \frac{14}{9} N_{\pi^0} \frac{b' e^{-b' p^+}}{p^+} dp^+ \int_{t=0}^{\ell} \int_{p^-=0}^{p^+} \exp\left[-\frac{1}{2}\left(\frac{\theta_{min}}{k\sqrt{t}} p_e\right)^2\right] dp_e\, dt . \qquad (A.8)$$

Since all of the scattering occurs for $p^- << p^+$, we can set the upper limit of the p^- integral to ∞ with negligible error, and we obtain from elementary integration

$$dN(e^+) = \frac{14}{9}\sqrt{\frac{\pi}{2}}\left(\frac{k}{p^+\theta_{min}}\right)\left(\frac{2}{3}\ell^{3/2}\right) e^{-b' p^+} (b' dp^+)\, N_{\pi^0} . \qquad (A.9)$$

We rewrite Eq. (A.9) in terms of the transverse momentum $p_T = p^+ \sin\theta$, and divide by the π^0 spectrum [Eq. (A.4)], in order to get the e/π ratio as a function of p_T, i.e.

$$\frac{e}{\pi} = \frac{14}{27}\sqrt{2\pi} \cdot \frac{k \sin\theta}{p_T \theta_{min}} \cdot \frac{1}{b p_T} \cdot \ell^{3/2} , \qquad (A.10)$$

where $\ell^{3/2}$ is the average (thickness)$^{3/2}$ of our vacuum tank. We abstract from Eq. (A.10) the dependence

$$\frac{e}{\pi} \propto \frac{k}{\theta_{min}} \times \frac{1}{p_T^2} . \qquad (A.11)$$

We use the $1/\theta_{min}$ dependence to correct the experimental data on pair production from the dummy wall for the fact that the dummy wall is several centimetres closer to the veto counters than the true vacuum tank wall, and hence, the number of pairs to be subtracted from the experimental total signal must be slightly ($\sim$ 9%) larger than the measured background. The experimental backgrounds due to γ-rays converting in the vacuum tank that are given in Table 1 have been corrected for this effect, using formula (A.11).

The $1/p_T^2$ behaviour, suggested by formula (A.11) for the idealized situation of a point source and a simplified Bethe-Heitler approximation, is well-confirmed by our Monte Carlo calculation, where we utilize the exact Bethe-Heitler law, the true vacuum chamber, a source of π^0's emerging from the ISR diamond with the proper spatial distribution, exact locations of guard counters, etc. The

approximate formula (A.10) agrees with the Monte Carlo results to an absolute precision of $\sim$ 35%, and thus Eq. (A.10) furnishes us with a reasonable analytic insight into the problem of pair-production background.

It should be noted that the use of the integral Gaussian law (A.1) to derive Eq. (A.11) is not essential and was made for the sake of simplicity. The same result can be arrived at in the same way, starting from any differential scattering law of the form $f(\theta)d\theta = g(\theta^2/\theta_0^2)\ d\theta/\theta_0$, where g is a normalized probability law, and $\theta_0 = k/p$.

APPENDIX B

CORRECTIONS FOR ELECTRON ENERGY LOSS DUE TO RADIATION

In the passage through the vacuum chamber and through the experimental apparatus, the electrons lose energy more rapidly than pions, because of bremsstrahlung. In order to correct the energy scale for the larger energy loss of electrons, we consider that electrons pass through a thickness of t radiation lengths (t = 0.083 up to the middle of the magnet). Electrons created with transverse momentum p_T will lose on the average a fraction t of their energy and their measured transverse momentum will be

$$p_T' = p_T(1 - t) \ . \tag{B.1}$$

If their initial spectrum was $n(p_T)\ dp_T$ their measured spectrum will be

$$n'(p_T')\ dp_T' = \frac{n(p_T)}{1 - t}\ dp_T' \ . \tag{B.2}$$

We use formulae (B.1) and (B.2) to correct our Monte Carlo calculated backgrounds (Dalitz pairs, K_{e3}) since the Monte Carlo program did not include energy loss due to radiation. If we fit the Monte Carlo results by $e/\pi \propto p_T^{-n}$ and insert the pion spectrum $N_\pi(p_T)\ dp_T \propto p_T\ e^{-bp_T}\ dp_T$, the corrected e/π ratio, $n'(p_T')/N_\pi(p_T')$, is easily shown to be given by:

$$\frac{e}{\pi}\ (\text{corrected}, p_T') = \frac{e}{\pi}\ (\text{uncorrected}, p_T')\ e^{-bp_Tt}\ (1 - t)^{n-2} \ . \tag{B.3}$$

To use this formula for estimating the corrections to the final data, we must correct upward, i.e. substitute -t for t in Eqs. (B.1) to (B.3). Using n = 1 as an approximate fit to our data in the small p_T region, we estimate that the corrections range from about 7% in the interval $0.2 \leq p_T \leq 0.3$ GeV/c to about +33% for the interval $0.8 \leq p_T \leq 0.9$ GeV/c. The e/π final data shown in Table 2 have not been corrected for this effect, and thus are slightly smaller than the true values.